Elevated Ornithine Decarboxylase Levels Activate Ataxia Telangiectasia Mutated–DNA Damage Signaling in Normal Keratinocytes

Gang Wei,[1] Karen DeFeo,[1] Candace S. Hayes,[1] Patrick M. Woster,[2] Laura Mandik-Nayak,[1] and Susan K. Gilmour[1]

[1]Lankenau Institute for Medical Research, Wynnewood, Pennsylvania and [2]Department of Pharmaceutical Sciences, Wayne State University, Detroit, Michigan

Abstract

We examined the effect of increased expression of ornithine decarboxylase (ODC), a key rate-limiting enzyme in polyamine biosynthesis, on cell survival in primary cultures of keratinocytes isolated from the skin of K6/ODC transgenic mice (Ker/ODC) and their normal littermates (Ker/Norm). Although elevated levels of ODC and polyamines stimulate proliferation of keratinocytes, Ker/ODC undergo apoptotic cell death within days of primary culture unlike Ker/Norm that continue to proliferate. Phosphorylation of ataxia telangiectasia mutated (ATM) and its substrate p53 are significantly induced both in Ker/ODC and in K6/ODC transgenic skin. Chromatin immunoprecipitation analyses show that the increased level of p53 in Ker/ODC is accompanied by increased recruitment of p53 to the *Bax* proximal promoter. ATM activation is polyamine dependent because α-difluoromethylornithine, a specific inhibitor of ODC activity, blocks its phosphorylation. Ker/ODC also displays increased generation of H_2O_2, acrolein-lysine conjugates, and protein oxidation products as well as polyamine-dependent DNA damage, as measured by the comet assay and the expression of the phosphorylated form of the histone variant γH2AX. Both reactive oxygen species generation and apoptotic cell death of Ker/ODC may, at least in part, be due to induction of a polyamine catabolic pathway that generates both H_2O_2 and cytotoxic aldehydes, because spermine oxidase (SMO) levels are induced in Ker/ODC. In addition, treatment with MDL 72,527, an inhibitor of SMO, blocks the production of H_2O_2 and increases the survival of Ker/ODC. These results show a novel activation of the ATM-DNA damage signaling pathway in response to increased ODC activity in nontumorigenic keratinocytes. [Cancer Res 2008;68(7):2214–22]

Introduction

Previous reports have shown that overexpression of ornithine decarboxylase (ODC) enzyme targeted to the skin of K6/ODC transgenic mice stimulates cellular proliferation in epithelial cells (1) and promotes the development of tumors in carcinogen-initiated skin (2). Although not sufficient to lead to tumor formation, overexpression of ODC in the skin of K6/ODC transgenic mice cooperates with oncogenes such as a mutated *H-ras* to produce spontaneous skin carcinomas in ODC/Ras double transgenic mice (3). Whereas elevated ODC activity provides a strong proliferative stimulus, it can also induce the expression of inhibitory proteins such as p53, $p21^{WAF1}$, and $p27^{KIP1}$ as well as evidence of apoptosis in nontumor-bearing skin of K6/ODC transgenic mice (1). Conversely, polyamine depletion via inhibition of ODC or the induction of polyamine catabolic enzymes leads to enhanced expression of inhibitory proteins and inhibition of cell proliferation as well (4–6). These observations support the little understood view that tightly regulated intracellular levels of polyamines are required to maintain cell growth and normal cellular homeostasis. Indeed, polyamines play an important role in a variety of cellular processes, including DNA replication, transcription, and translation.

Accumulation of p53 is unusual in normal nontumorigenic tissue because p53 has a short half-life and is normally maintained at low levels in unstressed mammalian cells. Levels of p53 protein are up-regulated in response to DNA damage and other cellular stress signals such as oncogenic signaling (7). Various forms of environmental and intracellular stress, including UV and ionizing radiation, DNA-damaging drugs, hypoxia, and hyperproliferation, rapidly induce a transient increase in p53 protein with little or no effect on the steady-state level of p53 mRNA (8). Although the function of the p53 protein has proven to be very intricate, it is generally agreed that an important function of p53 is to trigger apoptosis to ensure that damaged DNA is not propagated to daughter cells (7). Because of its pivotal role in cell cycle control, it is not surprising that the *p53* tumor suppressor gene is the most frequent target for genetic alterations in human cancers, with mutations occurring in almost 50% of all human tumors (9).

Ataxia telangiectasia mutated (ATM) kinase plays an essential role in maintaining genome integrity by coordinating cell cycle arrest, apoptosis, and DNA damage repair (10). DNA damage triggers the phosphorylation of ATM at serine 1981 (ATM $pSer^{1981}$), and this activation of ATM results in the subsequent phosphorylation of H2AX Ser^{139} (γH2AX) and p53 Ser^{15} (11, 12). The ATM-mediated phosphorylation of p53 inhibits Mdm2 binding and leads to accumulation and increased transcriptional activation capacity of p53 (11). Recent reports have shown that the ATM-DNA damage response pathways are activated early by a number of proliferative or oncogenic factors, such as Myc, E2F1, and cyclin E (13–15).

This study investigates the apparent contradiction of the widely accepted role of ODC as a strong tumor-promoting stimulus with the induction of cell death in a normal epithelial cell type that express elevated levels of ODC. We show that elevated ODC activity and increased biosynthesis of polyamines serve as a novel stimulus to induce the ATM-DNA damage signaling pathway and cell death in normal keratinocytes.

Requests for reprints: Susan K. Gilmour, Lankenau Institute for Medical Research, 100 Lancaster Avenue, Wynnewood, PA 19096. Phone: 610-645-8429; Fax: 610-645-2205; E-mail: gilmours@mlhs.org.

doi:10.1158/0008-5472.CAN-07-5030

Materials and Methods

Transgenic animals. K6/ODC transgenic mice in which a keratin 6 promoter directs the expression of ODC to the outer root sheath cells of hair follicles in the skin were used as previously described (1–3). K6/ODC transgenic mice were bred with $p53^{-/-}$ mice (obtained from The Jackson Laboratory) to generate $p53^{-/-}$ mice that express the ODC transgene.

Primary cultures of epidermal cells. Primary cultures of epidermal cells were isolated from 3- to 4-d-old K6/ODC transgenic newborn pups and their normal littermates by a trypsin flotation procedure. K6/ODC transgenic pups were distinguished from their normal littermates by PCR genotyping for the K6/ODC transgene. Cells were plated at 3.2×10^6 per 60-mm dish or onto glass coverslips in low calcium keratinocyte medium (EMEM without calcium, Cambrex) supplemented with 8% chelex-treated fetal bovine serum, 0.05 mmol/L calcium, epidermal growth factor, aminoguanidine, and gentamicin, and grown at 35°C with 5% CO_2. Some cells were treated with 3 mmol/L α-difluoromethylornithine (DFMO) or 25 μmol/L *N,N′*-bis(2,3-butadienyl)-1,4-butanediamine (MDL 72,527) after plating. DFMO was obtained from ILEX Oncology, and MDL 72,527 was synthesized in the laboratory of Dr. Patrick Woster.

Protein extraction and immunoblot analyses. Keratinocytes were homogenized in either radioimmunoprecipitation assay buffer [RIPA; 50 mmol/L Tris-HCl (pH 7.4); 150 mmol/L NaCl; 0.25% (w/v) deoxycholic acid; 1% (w/v) NP40; 1 mmol/L EDTA, containing 1 μg/mL each of aprotonin, leupeptin, pepstatin, 1 mmol/L sodium orthovanadate, 1 mmol/L sodium fluoride, and 1 mmol/L Pefabloc], or Laemmli buffer [125 mmol/L Tris-HCl (pH 6.8); 20% glycerol; and 4% SDS, containing the same protease inhibitors as RIPA buffer] and passed through a syringe needle multiple times preceding a 45-min incubation on ice. Lysates were clarified by centrifugation at 14,000× *g* for 10 min and the protein content was determined using the Bio-Rad D/C protein assay kit (Bio-Rad Laboratories). Nuclear extracts were prepared using NE-PER kit (Pierce). Total skin tissues excised from K6/ODC transgenic and normal littermate mice were frozen in liquid nitrogen, pulverized, and stored at −80°C. Ground skin tissue was homogenized in RIPA-DTT buffer [50 mmol/L Tris-HCl (pH 7.5), 1% NP40, 0.25% sodium deoxycholate, 0.25% SDS, 150 mmol/L NaCl, 1 mmol/L EGTA, and 1 mmol/L DTT] containing 2 μg/μL each of aprotinin, leupeptin, and pepstatin, 1 mmol/L sodium fluoride, 1 mmol/L sodium orthovanadate, and 1 mmol/L Pefabloc, by passing through a syringe needle and incubating 30 min on ice. Debris was removed by centrifugation at 13,000 rpm for 10 min. Protein content was determined using the Bio-Rad D/C protein assay kit.

Protein lysates were separated by SDS-PAGE, transferred to polyvinylidene difluoride (PVDF) membranes (Millipore), and briefly stained with Ponceau S (Sigma) to verify efficient transfer. Immunoblots were incubated overnight at 4°C in blocking solution (PBS with 5% nonfat dry milk and 0.05% Tween 20) followed by 2-h incubation with the primary antibody diluted in PBS-Tween. Blots were probed with antibodies directed against proliferating cell nuclear antigen (PCNA), Lamin B, and p21 (Santa Cruz Biotechnology); p53 and phospho-p53 (Ser^{15}; Cell Signaling Technology); phospho-ATM (Ser^{1981}; Rockland); ATM (Genetex, Inc.); phospho-histone H2AX (Ser^{139}), Bax, and Bcl-2 (Upstate Biotechnology); $p19^{ARF}$ (Calbiochem); and spermine oxidase (SMO; a kind gift from Bob Casero, Johns Hopkins University, Baltimore, MD) were used with the appropriate secondary antibody conjugated to horseradish peroxidase. Antibody binding was detected by enhanced chemiluminescence (ECL Plus Western Blotting Detection System, Amersham/GE Healthcare). Filters were reprobed with an antibody against tubulin (Calbiochem) to verify equal loading of protein.

Immunofluorescence. Formaldehyde-fixed, paraffin-embedded mouse skin sections were deparaffinized, steamed in 0.1 mmol/L sodium citrate (pH 6.0) for 10 min, and incubated overnight at 4°C with antibodies specific for ATM pS1981 (Rockland Immunochemicals, Inc.) or ATM (GeneTex), followed by incubation with secondary antibody conjugated to Cy3 (Jackson ImmunoResearch Laboratories). Sections were covered with coverslips mounted with Vectashield mounting medium containing 4′,6-diamidino-2-phenylindole (DAPI; Vector Laboratories) to counterstain DNA and to visualize the nuclei of all cells. Immunostained sections were imaged by fluorescence microscopy using a Zeiss Axioplan microscope powered by Axiovision 3.1 software and an Axiocam digital camera.

Single-cell gel electrophoresis (comet) assay. Primary keratinocytes, at a concentration of 2×10^5 cells/mL, were embedded in low-melting-point agarose on a glass slide using the Comet Assay kit and the manufacturer's protocol (Trevigen). The embedded cells were incubated overnight at 4°C in the lysis solution provided. The following morning, slides were incubated in alkaline solution for 40 min to denature the DNA. The samples were then washed twice in Tris-borate EDTA (TBE) buffer and electrophoresed at 19 V for 10 min in 1× TBE buffer. The samples were stained with 50 μL of SYBR Green, and nuclei were visualized by fluorescent microscopy. Tail length and olive tail moment of at least 250 nuclei were scored using the Cometscore software (TriTek; Student's *t* test was used to derive *P* values). Tail moment is the product of the tail length and the fraction of total DNA in the tail, which gives a measure of the extent of DNA damage.

Detection of reactive oxygen species. Cells were trypsinized, collected in PBS, and spun down for 4 min at 1,000 rpm at 4°C. H_2O_2 generation was determined by incubating the cells with 10 μmol/L CM-H_2DCFdA (Molecular Probes) in 0.8 mL PBS at 37°C on a nutator for 25 min. Samples were spun again for 4 min at 1,000 rpm at 4°C and resuspended in 1 mL of PBS before being immediately read on a BD FACSCanto II flow cytometer and analyzed using BD FACS Diva software (Becton Dickinson).

Detection of oxidative proteins and acrolein-conjugated proteins. The Oxyblot protein oxidation detection kit (Chemicon), based on the reaction of protein carbonyl groups with 2,4-dinitrophenylhydrazine, was used to perform the assay following the manufacturer's directions. For detection of acrolein-conjugated protein, PBS cell lysates were assayed by a direct NWLSS ACRL01 ELISA using a monoclonal antibody to acrolein-lysine (Northwest Life Science Specialties).

Immunohistochemistry. Primary keratinocytes grown on glass coverslips were washed with cold PBS and fixed for 20 min with 4% *p*-formaldehyde in PBS. Slides were incubated with a primary antibody specific to the p20 subunit of caspase-3 (R&D Systems). Slides were then incubated with a biotinylated secondary antibody and then with an avidin-biotinylated horseradish peroxidase complex (Vectastain Elite ABC kit, Vector Laboratories). Immunoreactive cells were detected using diaminobenzidine chromagen solution and then counterstained with hematoxylin. At least 1,000 cells were counted for each group and the percentage of stained cells was reported.

Chromatin immunoprecipitation analysis. Experiments were performed using the Chromatin Immunoprecipitation Assay Kit (Upstate Biotechnology, Inc.) with some modification. Cells were fixed in 1% formaldehyde in PBS and rotated at room temperature for 15 min. The cross-linking reaction was stopped by adding glycine to a final concentration of 0.125 mol/L with continued rotation for 5 min. Samples were centrifuged at low speed, washed once with cold PBS, incubated in PIPES buffer [5 mmol/L Pipes (pH 8.0), 85 mmol/L KCl, 0.5% NP40, 10 mmol/L sodium butyrate, and inhibitor cocktail] on ice for 10 min, and homogenized on ice using a polytron homogenizer. Following low-speed centrifugation, the pellet was resuspended in nuclei lysis buffer [50 mmol/L Tris-HCl (pH 8.1), 10 mmol/L EDTA, 1% SDS and inhibitors], incubated on ice for 20 min, and centrifuged. The pelleted material was resuspended in chromatin immunoprecipitation (ChIP) lysis buffer and the chromatin was sonicated to an average length of 800 to 600 bp. After clearance by centrifugation at maximum speed for 10 min at 4°C, the supernatant was diluted 10-fold in ChIP dilution buffer and incubated with salmon sperm DNA/protein A agarose for 30 min at 4°C with agitation. The precleared lysate was then incubated with polyclonal antibody p53 (FL-393) at 4°C overnight. The immunocomplexes were captured by salmon sperm DNA adsorbed/protein A beads. After sequential washings, the immunocomplexes were eluted from the beads, and DNA-protein cross-links were reversed by incubating for 6 h at 65°C. DNA was purified using the MinElute PCR cleanup kit (Qiagen). The following primers were used to amplify the proximal promoter of the *Bax* gene: sense primer 5′-GATGTTGTAGCCACCGCGTACAGCC-3′; antisense primer 5′-TTCATGGTA-GAGAGCACTAAGGAGG-3′.

RNA isolation and reverse transcription-PCR. Total RNA was isolated from skin tissue using TriReagent (Molecular Research Center). Total RNA (2 μg) was reverse transcribed using random hexamer primers at 42°C for 1 h. Duplicate PCR amplification reactions contained 200 μmol/L deoxynucleotide triphosphates, 0.04 to 0.5 μmol/L forward and reverse primers, 1 mol/L betaine, and 1 unit of polymerase. A constitutively expressed gene, *glyceraldehyde 3-phosphate dehydrogenase* (*GAPDH*), was simultaneously amplified as an internal control. Twenty microliters of PCR products were electrophoresed on a 1.5% agarose gel. The primers used for PCR were SMO forward primer 5′-CACGTGATTGTGACCGTTTC-3′and reverse primer 5′-TGGGTAGGTGAGGGTACAGTC-3′; spermidine/spermine N^1-acetyltransferase (SSAT) forward primer 5′-GACCCCTGAAGGACATAGCA-3′ and reverse primer 5′-CCGAAGCACCTCTTCTTTTG-3′; acetylpolyamine oxidase (APAO) forward primer 5′-CTTTTCCAGGGGAGACCTTC-3′ and reverse primer 5′-CACACCACCTGGATGAACTG-3′; *S*-adenosylmethionine decarboxylase (AdoMetDC) forward primer 5′-GACATTAGCTAGCGCTCGCTCAAC-3′ and reverse primer 5′-CAGACCTCCAGCAGTTTCTCCGTCCCTTCG-3′; and GAPDH forward primer 5′-TGCTGAGTATGTCGTGGAGTC-3′ and reverse primer 5′-AGTGGGAGTTGCTGTTGAAGT-3′.

Results

Polyamine-dependent p53 protein accumulation and apoptotic cell death in ODC-overexpressing primary keratinocytes. To investigate the effect of elevated ODC activity on normal epithelial cell function, we cultured primary keratinocytes from the skin of K6/ODC transgenic mice (Ker/ODC) and their normal littermates (Ker/Norm). In agreement with previous reports that increased ODC activity directed to various subpopulations of epidermal cells stimulates cell proliferation both *in vivo* (1, 16) and in primary keratinocyte cultures (16), the proliferation marker PCNA remains elevated in Ker/ODC (Fig. 1*A*). However, expression of proteins associated with cell growth inhibition, such as p53 and $p21^{Waf1}$, also increases in Ker/ODC compared with Ker/Norm (Fig. 1*A*). Treatment with DFMO prevents these changes in Ker/ODC and normalizes the cells. Indeed, Ker/ODC undergo early cell death within a week of culture unlike Ker/Norm that remained viable (Fig. 1*B*). Viability of Ker/ODC seems to be dependent on cell density because plating both Ker/ODC and Ker/Norm at near-confluent density prolongs the survival of Ker/ODC, albeit only delaying the earlier death of Ker/ODC compared with that of Ker/Norm. This early cell death is dependent on polyamine biosynthesis because treatment of Ker/ODC with DFMO, a specific inhibitor of ODC enzyme activity, blocks cell death. Cell death in ODC-overexpressing keratinocytes seems to be due to apoptosis as evidenced by a significant increase in numbers of Ker/ODC positive for the activated cleaved form of caspase-3 compared with that

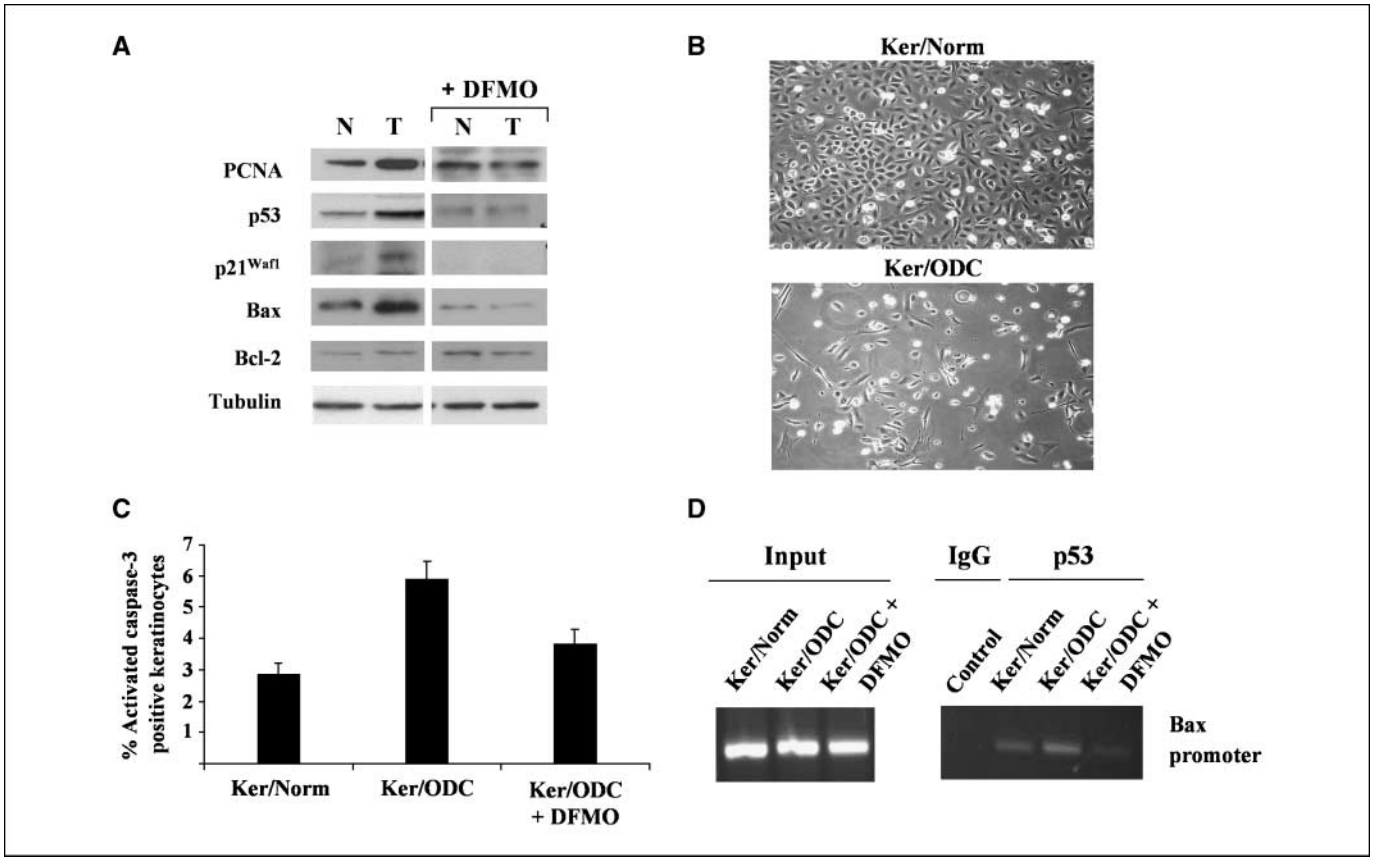

Figure 1. Polyamine-dependent p53 protein accumulation and apoptotic cell death in ODC-overexpressing primary keratinocytes. Primary keratinocytes were isolated from K6/ODC transgenic mice (*T*) and their normal littermates (*N*) and plated. Some of the K6/ODC keratinocytes were treated with 3 mmol/L DFMO. *A,* after 5 d in culture, cells were harvested in RIPA buffer and equal amounts of protein were resolved by SDS-PAGE and transferred to PVDF membranes. PCNA, p53, $p21^{Waf1}$, Bax, and Bcl-2 were detected by immunoblotting, and the membranes were reprobed for tubulin protein as a loading control. *B,* representative photomicrographs of Ker/Norm and Ker/ODC following 6 d in culture. *C,* keratinocytes were stained immunohistochemically using an anti–caspase-3 (active form) antibody. The values for the percent caspase-3–stained keratinocytes are the percentages of caspase-3–stained cells out of the total cells per coverslip. At least 1,000 total cells were counted per group. *D,* the *Bax* promoter was assessed by ChIP analysis for p53 binding in cross-linked protein-DNA complexes precipitated from Ker/Norm, Ker/ODC, and Ker/ODC + DFMO–treated keratinocytes using an anti-p53 antibody or rabbit IgG as a control. PCR was performed with primers specific for the *Bax* promoter, which included the p53 binding site. To verify equal amounts of starting material, PCR was performed on aliquots of the chromatin removed before immunoprecipitation (*Input*). Amplified DNA was visualized by agarose gel electrophoresis.

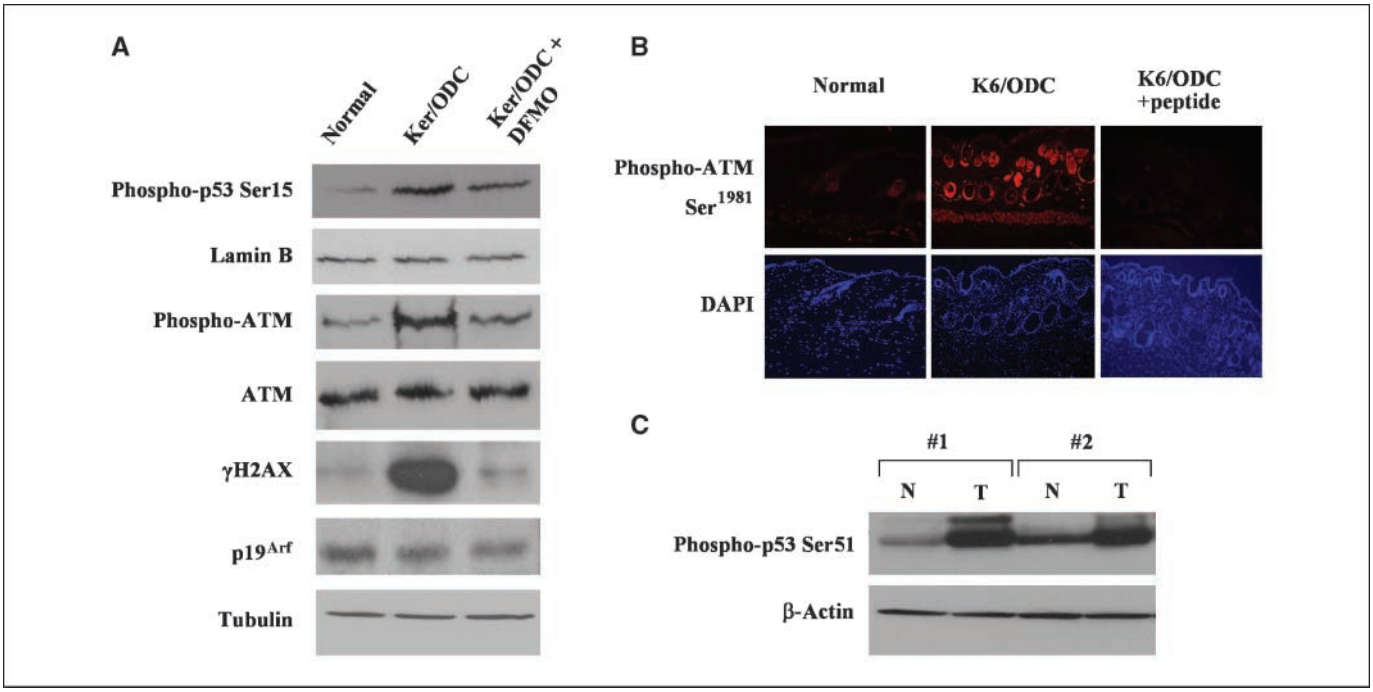

Figure 2. ODC overexpression activates ATM in primary keratinocytes and in K6/ODC transgenic skin. *A,* primary keratinocytes were isolated from K6/ODC transgenic mice (*Ker/ODC*) and their normal littermates (*Ker/Norm*) and plated. Some of the Ker/ODC were treated with 3 mmol/L DFMO. Nuclear extracts and RIPA lysates were prepared and equal amounts of protein were resolved by SDS-PAGE and transferred to PVDF membranes. Nuclear extracts were probed for phospho-p53 (Ser^{15}) and lamin B. Total cellular lysates were probed for ATM, γH2AX, and $p19^{Arf}$ by immunoblotting and then reprobed for tubulin protein as a loading control. *B,* immunofluorescence of normal littermate skin and K6/ODC transgenic mouse skin using an antibody specific for ATM phosphorylated at serine-1981 (pATM) in the presence or absence of a peptide for ATM phosphorylated at Ser^{1981}. DAPI was used for the same views to identify all nuclei. *C,* normal and K6/ODC skins were resolved by SDS-PAGE, transferred to PVDF, and probed for phospho-p53 (Ser^{15}) and β-actin by immunoblotting.

seen in Ker/Norm or in DFMO-treated Ker/ODC (Fig. 1*C*). In addition, the expression of the proapoptotic protein, Bax, increased in Ker/ODC with no significant change in the prosurvival protein Bcl-2, and this was prevented when Ker/ODC were cultured in medium containing DFMO to inhibit ODC activity (Fig. 1*A*).

To confirm whether accumulated and, therefore stabilized, p53 may be regulating the expression of the proapoptotic gene *Bax*, we investigated whether more p53 is bound to the Bax promoter using cross-linked chromatin from Ker/Norm, Ker/ODC, and DFMO-treated Ker/ODC using a ChIP assay. Figure 1*D* shows enhanced binding of p53 protein to the *Bax* promoter in ODC-overexpressing keratinocytes and the inhibition of this binding in Ker/ODC treated with DFMO. These findings suggest that polyamine-dependent p53 accumulation plays a role in the induction of apoptosis in ODC-overexpressing keratinocytes.

ODC overexpression activates ATM in the DNA damage signaling pathway. Posttranslational modification of p53, including phosphorylation, plays an essential role in both stabilization and activation of the normally short-lived p53 protein (11, 17). Because p53 protein accumulates in keratinocytes with elevated ODC activity, we analyzed nuclear extracts of Ker/ODC and Ker/Norm for p53 phosphorylated at Ser^{15}. Phosphorylation of Ser^{15} in p53 was induced in Ker/ODC, and the ODC induction of p53 phosphorylation was blocked by DFMO (Fig. 2*A*). There was no change in lamin B, indicating equal extraction of nuclear protein. Phosphorylation and activation of ATM leads to the phosphorylation of several ATM targets, including Ser^{15} in p53 as well as Mdm2 and γH2AX, the phosphorylated form of the histone variant H2AX (18). Immunoblot analyses of cell lysates from Ker/ODC and Ker/Norm revealed not only elevated phosphorylation of ATM at Ser^{1981} but also increased phosphorylation of the ATM substrate, γH2AX (Fig. 2*A*) and Mdm2 (data not shown). Similar to p53 phosphorylation, DFMO treatment suppressed both the ATM and γH2AX phosphorylation, indicating that elevated levels of ODC leads to ATM activation and subsequent phosphorylation and activation of p53.

Stabilization of p53 can also be mediated through the Arf-mdm2-p53 pathway that is activated by growth-promoting stimuli such as oncoproteins. For example, constitutive and simultaneous activation of multiple signaling pathways by oncogenic Myc induces $p19^{ARF}$, which blocks Mdm2-mediated inhibition of p53 and stabilizes p53 (19). Although ODC is transactivated by c-Myc, immunoblot analyses revealed no change in the levels of $p19^{Arf}$ expression in Ker/ODC compared with Ker/Norm (Fig. 2*A*).

To determine if elevated polyamine biosynthesis activates the ATM pathway *in vivo*, we examined the skin of K6/ODC transgenic mice, in which ODC is targeted to the outer root sheath cells of hair follicles with a keratin 6 promoter (1). Immunofluorescent staining was performed on skin sections from K6/ODC transgenic mice and their normal littermates. ATM phosphorylated at Ser^{1891} was detected in the epithelial cells lining follicular cysts in the dermis of K6/ODC transgenic skin (Fig. 2*B*), which corresponds to the staining pattern for ODC protein. Phospho-ATM staining was completely inhibited with the addition of phospho-ATM peptide (Fig. 2*B*). In contrast, there was no significant difference in the ATM staining pattern in skin sections from K6/ODC transgenic mice and normal littermates (data not shown). Phosphorylation of

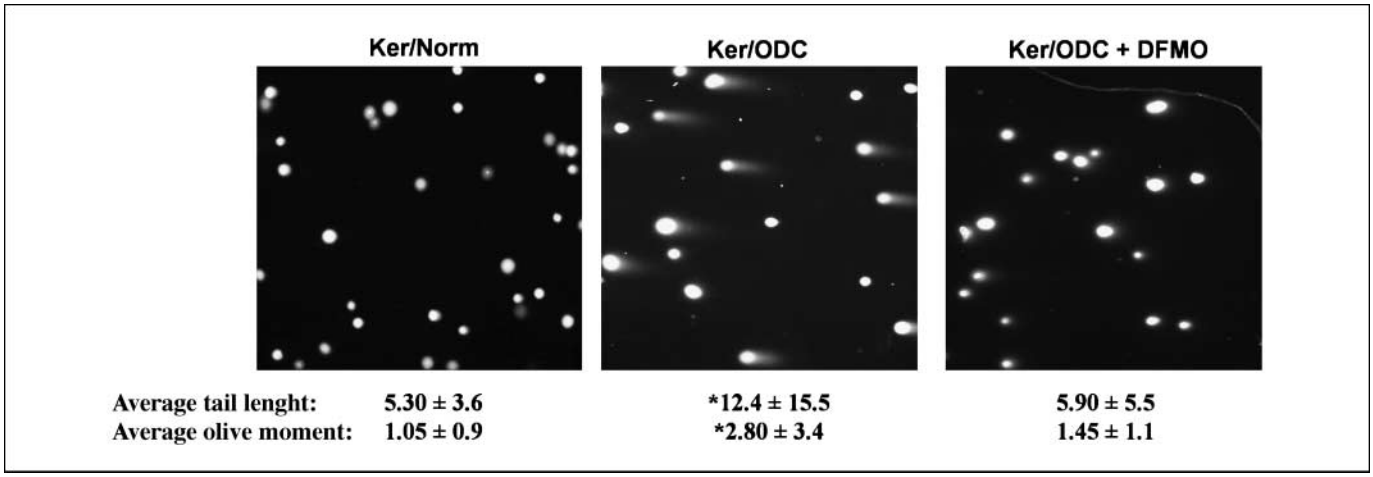

Figure 3. DNA damage induced by elevated ODC activity in primary keratinocytes. Primary keratinocytes were isolated from K6/ODC transgenic mice (*Ker/ODC*) and their normal littermates (*Ker/Norm*) and plated. Some of the Ker/ODC were treated with 3 mmol/L DFMO. Following 5 d in culture, keratinocytes were harvested, embedded in low-melting-point agarose, and processed for the alkaline comet assay as described in Materials and Methods. Each slide was stained with SYBR Green, photographed using a fluorescent microscope, and the average tail lengths ± SD were scored and analyzed using the Cometscore software to determine the average olive moments ± SD. *, $P < 0.0001$, significantly different compared with Ker/Norm or with DFMO-treated Ker/ODC.

Ser[15] in p53 was significantly induced in K6/ODC transgenic skin compared with normal littermate skin (Fig. 2*C*). These combined results suggest that elevated ODC is a novel stress signal that activates the ATM response pathway.

DNA damage induced by elevated ODC activity in primary keratinocytes. Whereas γH2AX has been reported to be a sensitive marker for detecting DNA damage (20), the Comet assay was also used to confirm that elevated ODC activity in primary cultures of keratinocytes induces DNA damage. In contrast to wild-type keratinocytes, the majority of Ker/ODC showed comet tails, indicating DNA damage (Fig. 3). Although some tails were also detected in DFMO-treated Ker/ODC, the number of positive cells and the average length of the comet tails were similar to that seen with Ker/Norm and significantly depressed compared with non-treated Ker/ODC. Measurements of the average tail length and tail moment confirmed that Ker/ODC had significantly ($P < 0.0001$)

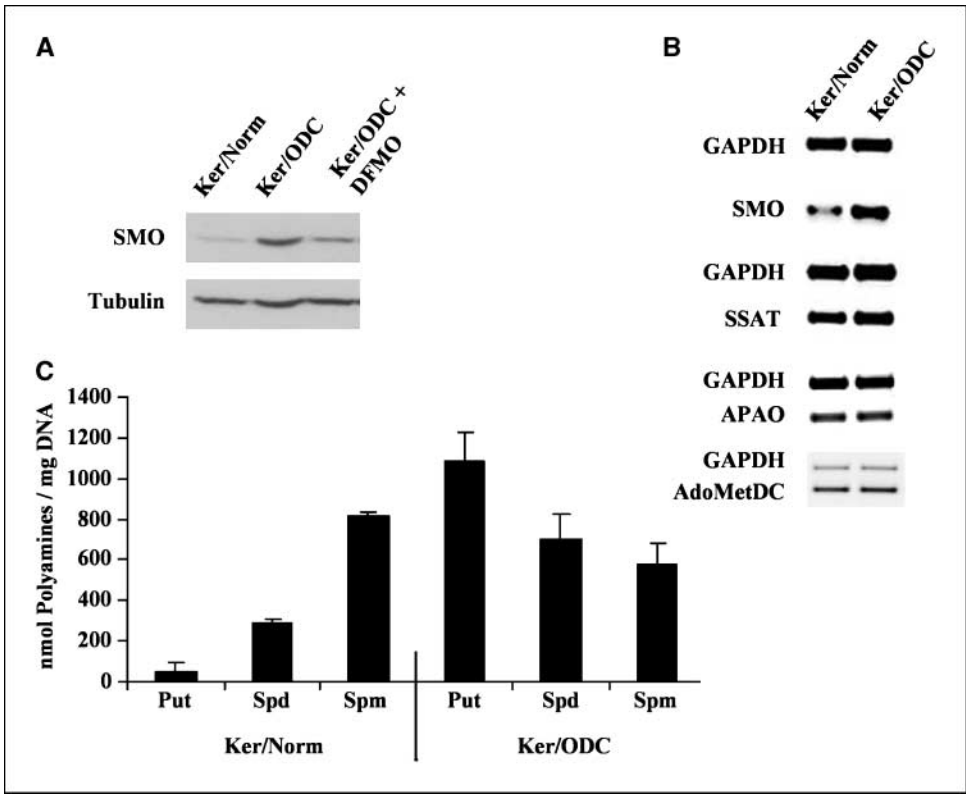

Figure 4. Elevated ODC activity induces SMO. *A,* after 3 d in culture, Ker/Norm, Ker/ODC, and Ker/ODC treated with 3 mmol/L DFMO were harvested. Immunoblot analysis of total cellular protein lysates in which blots were probed with an antibody specific for SMO and reprobed for tubulin as a control. *B,* RNA was prepared from Ker/Norm and Ker/ODC 3 d after isolation from the skin of K6/ODC transgenic mice and their normal littermates. RT-PCR was performed to analyze levels of SMO, SSAT, APAO, and AdoMetDC at the mRNA level. GAPDH mRNA was simultaneously monitored as an internal PCR control for each reaction. *C,* high-performance liquid chromatography analyses of total intracellular polyamine levels in Ker/Norm and Ker/ODC harvested 3 d in culture. Polyamines (*Put,* putrescine; *Spd,* spermidine; *Spm,* spermine) are expressed in nmol/mg DNA. *Bars,* SD.

more DNA damage compared with normal littermate keratinocytes and that inhibition of polyamine biosynthesis with DFMO blocked the induction of DNA damage (Fig. 3).

Increased reactive oxygen species with elevated ODC activity. The induction of polyamine catabolic pathways leads to the production of H_2O_2 and cytotoxic aldehydes (6, 21). The back conversion of the polyamines spermine and spermidine can be mediated by two pathways, both involving oxidases that generate H_2O_2 (22–25). Spermine can be directly converted to spermidine, H_2O_2, and 3-aminopropanal by SMO. In addition, spermine or spermidine can first be acetylated by SSAT and then oxidized by APAO to produce H_2O_2 as a by-product. The effect of elevated ODC activity on possible induction of SMO, SSAT, and APAO mRNA was examined using semiquantitative reverse transcription-PCR (RT-PCR). Although SSAT and APAO mRNA were not induced in Ker/ODC, SMO mRNA levels were elevated in keratinocytes with increased ODC activity (Fig. 4*B*). Immunoblot analyses of keratinocyte lysates revealed that SMO protein is induced in ODC-overexpressing keratinocytes and inhibited with DFMO (Fig. 4*A*). However, we found no evidence of increased APAO protein levels or increased SSAT activity in Ker/ODC compared with Ker/Norm (data not shown). Moreover, although high-performance liquid chromatography analysis of intracellular polyamines revealed increased levels of putrescine in Ker/ODC, acetylated polyamines were not detected and spermine levels were decreased (Fig. 4*C*). Consistent with the small increase in spermidine and the lack of increase in spermine levels in Ker/ODC, we found no increased expression of AdoMetDC, the rate-limiting enzyme in the biosynthesis of spermidine and spermine (Fig. 4*B*). These data suggest that increased ODC activity results in dramatic increases in putrescine levels and reduced spermine levels due to induction of the catabolic enzyme SMO.

Because reactive oxygen species (ROS) induce oxidative damage of DNA, resulting in DNA breaks that can activate the ATM-DNA damage response pathway (26, 27), we investigated whether ROS play a role in the activation of the ATM-DNA damage pathway in ODC-overexpressing primary keratinocytes. ROS activity was measured in Ker/Norm and Ker/ODC via fluorescence measured by flow cytometry. Figure 5*A* shows a significant increase in the ROS production as indicated by the shift to the right of the fluorescence peaks in the presence of CM-H_2DCFDA, an oxidation-sensitive fluorescent probe. Spermine oxidation by SMO produces H_2O_2 and 3-aminopropanal that spontaneously forms the highly reactive and toxic compound acrolein (28). Protein-conjugated acrolein levels as determined by ELISA assay were significantly elevated in Ker/ODC compared with Ker/Norm, and the accumulation of acrolein protein conjugates was prevented with DFMO treatment (Fig. 5*B*). Additional evidence of ROS production included a 2-fold increase in protein carbonyl levels, or protein oxidation products, in Ker/ODC lysates compared with that of Ker/Norm or DFMO-treated Ker/ODC (Fig. 5*C*). Altogether, these results suggest that elevated ODC activity induces spermine catabolism via SMO, subsequently leading to increased ROS activity in primary cultures of keratinocytes.

Inhibition of ODC or polyamine catabolic enzymes increases survival of ODC overexpressing keratinocytes. To determine if polyamine catabolism is the source of ODC-induced H_2O_2 production, Ker/ODC were cultured with MDL 72,527, an inhibitor of the polyamine catabolic enzymes SMO and polyamine oxidase (25). Similar to culture with DFMO, treatment with 25 μmol/L MDL 72,527 attenuated the shift to the right in fluorescence in the presence of CM-H_2DCFDS in Ker/ODC compared with Ker/Norm

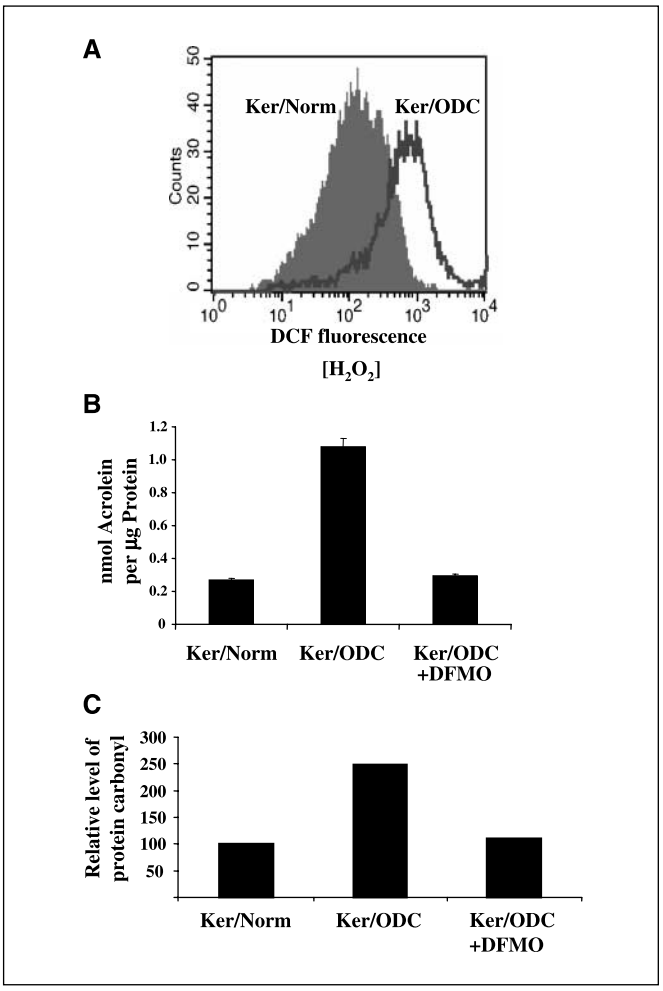

Figure 5. Elevated ODC activity leads to increased ROS generation. *A,* the levels of H_2O_2 production in Ker/Norm and Ker/ODC were compared using flow cytometry. Four days following culture, cells were incubated with 10 μmol/L CM-H_2DCFdA at 37°C for 25 min, and fluorescence was measured using a BD FACS Canto II flow cytometer. *X axis,* fluorescent intensity; *Y axis,* cell number. Representative results of four experiments that gave similar results. *B,* 4 d following culture, Ker/Norm, Ker/ODC, and Ker/ODC treated with 3 mmol/L DFMO were harvested by freeze-thaw in PBS and nmol acrolein-lysine conjugates/mg protein was determined by direct ELISA assay. *Bars,* SD. *C,* relative level of protein carbonyl groups in Ker/Norm, Ker/ODC, and Ker/ODC treated with 3 mmol/L DFMO was measured using an Oxyblot protein oxidation kit after proteins were resolved by SDS-PAGE and transferred to PVDF.

(Fig. 6*A*). Because MDL 72,527 inhibits ROS generation in Ker/ODC, the cells were cultured with MDL 72,527 to compare their survival with nontreated Ker/ODC. Most of the ODC-overexpressing keratinocytes died by 7 days following plating, but the Ker/ODC treated with MDL 72,527 remained viable similar to the Ker/Norm- or DFMO-treated Ker/ODC even after 2 weeks in culture (Fig. 6*B*). Thus, MDL 72,527 inhibition of polyamine catabolic oxidase activity and its associated generation of ROS prevent the early apoptotic death of ODC-overexpressing keratinocytes.

In an attempt to determine whether the ODC-induced apoptosis of primary keratinocytes is p53 dependent, K6/ODC transgenic mice were bred with $p53^{-/-}$ knockout mice. Primary keratinocytes were cultured from the skin of $p53^{-/-}$ knockout mice in which the ODC transgene is expressed and compared with $p53^{-/-}$ keratinocytes with no ODC transgene expression. Both Ker/ODC and Ker/Norm with $p53^{-/-}$ continued to proliferate 2 weeks following

plating (Fig. 6*B, bottom*) unlike the Ker/ODC with wild-type p53 that all died by 7 days of cell culture (Fig. 6*B, top right*). Thus, these data show that loss of p53 function confers increased survival in Ker/ODC.

Discussion

Although ATM is stimulated in response to a variety of oncogenic signals and DNA damage (29), we show that elevated levels of ODC activity stimulate ROS production and the ATM-DNA damage response pathway leading to apoptotic cell death of nontumorigenic epithelial cells. Our studies with primary keratinocytes isolated from $p53^{-/-}$ null mice show that a loss of p53 function confers increased survival in Ker/ODC, suggesting that the ODC induction of cell death in primary keratinocytes is p53 dependent. Normal cells are well protected against malignant transformation by the tumor suppressive activity of p53 that regulates the transcription of genes required for cell cycle arrest, DNA repair, and apoptosis. In addition to DNA damage, oncogenic signaling activates p53 through ARF, which interacts with MDM2 to inhibit its p53 ubiquitin ligase activity (19). However, we found no evidence of increased expression of $p19^{Arf}$ in primary keratinocytes with elevated ODC. Our studies show that the activation of ATM and phosphorylation of the ATM substrates p53 and γH2AX are induced in both K6/ODC transgenic skin and in ODC-overexpressing primary keratinocytes. In addition, previous studies have shown that levels of the Tip60 HAT enzyme, reported to acetylate and activate ATM (30), are also substantially elevated in the skin of ODC-overexpressing mice (31).

Because oncogenes such as *c-Myc* can transactivate and up-regulate ODC expression (32), it is possible that activation of ATM by oncogenes such as *c-Myc* (15) is, at least in part, due to

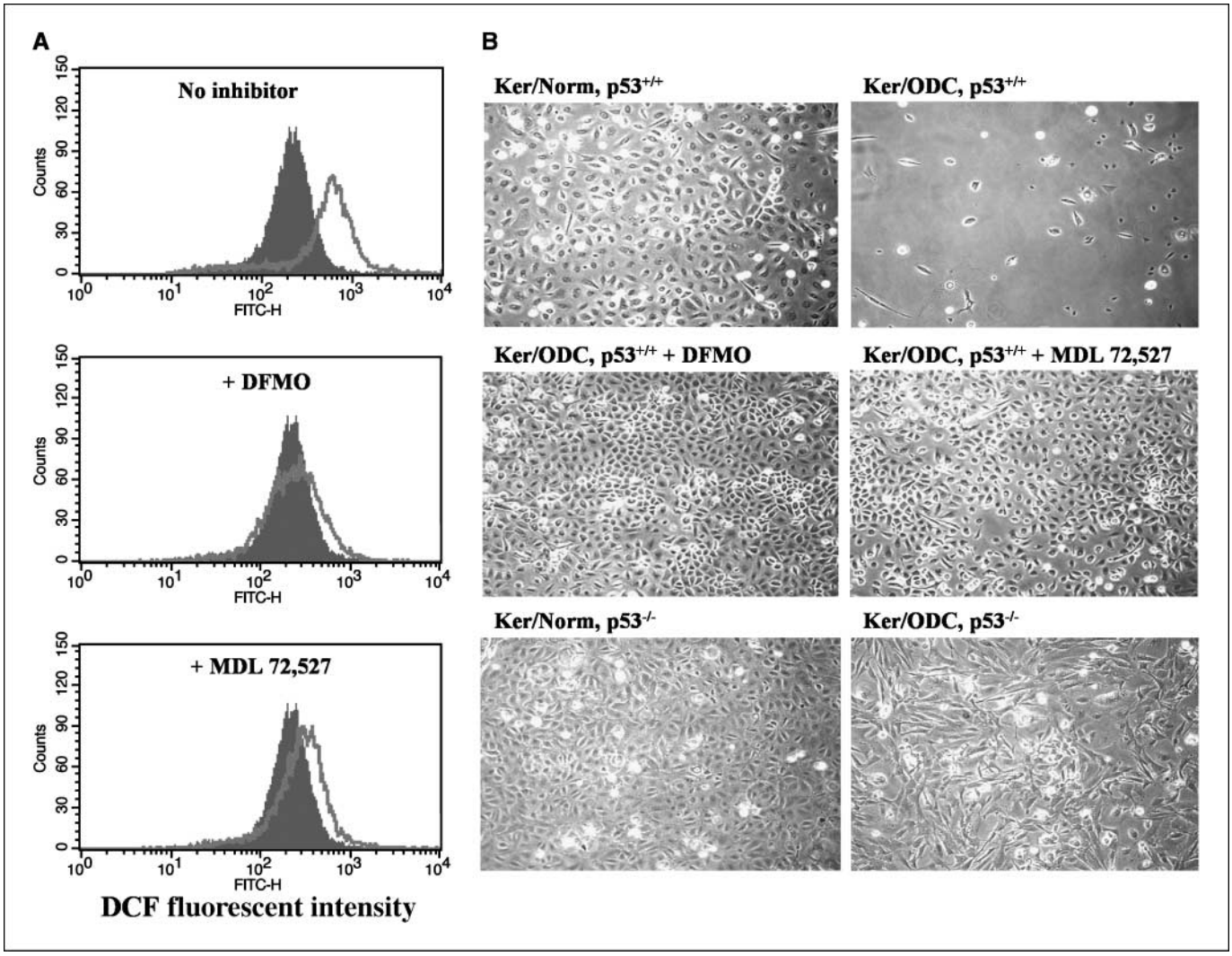

Figure 6. DFMO and MDL 72,527 prevent H_2O_2 generation in primary keratinocytes and increase survival of Ker/ODC. Primary keratinocytes were isolated from K6/ODC transgenic mice and their normal littermates as well as from K6/ODC transgenic mice and normal littermates bred to a $p53^{-/-}$ background. Some Ker/ODC were cultured with 3 mmol/L DFMO or 25 μmol/L MDL 72,527 in the medium. *A,* the levels of H_2O_2 production in Ker/Norm (*shaded curve*) and Ker/ODC (*open curve*) treated with and without 3 mmol/L DFMO and 25 μmol/L MDL 72,527 were compared using flow cytometry. Four days following culture, cells were incubated with 10 μmol/L CM-H_2DCFdA at 37°C for 25 min, and fluorescence was measured using a BD FACS Canto II flow cytometer. *X axis,* fluorescent intensity; *Y axis,* cell number. *B,* representative phase contrast images were taken of the keratinocytes after 14 d in culture to capture the difference in survival between Ker/Norm and Ker/ODC treated with and without 3 mmol/L DFMO and 25 μmol/L MDL 72,527. Whereas no viable Ker/ODC, $p53^{+/+}$ remained by 7 d in culture, Ker/ODC, $p53^{-/-}$ were still proliferating after 14 d of culture.

increased polyamine metabolism and production of ROS and DNA damage. This study adds ODC to the list of growth-promoting stimuli, including oncogenes such as *Myc* or *E2F1*, which have been reported to induce the ATM signaling pathway (13, 15). DNA replication stress has been suggested to be a trigger for the ATM response pathway, which has been found to be activated in precancerous lesions (33, 34). Oncogenic activation may generate DNA damage through the production of ROS and/or through the aberrant firing of replication origins (13, 35, 36). That elevated polyamine biosynthesis acts as a strong proliferative and tumor-promoting stimulus while also inducing p53-mediated tumor suppressive activity presents a seeming paradox. However, a similar precedence has been reported for a variety of proliferative signals, including the oncogenes *c-Myc, Ras*, and *E2F1* (13, 15, 37). Although the immediate result is protective via cell cycle arrest and apoptosis of aberrantly growing cells that still retain a functional p53 (Fig. 6), it can also create a selection pressure for inactivation of ATM or p53, thus leading to genetic instability and tumor progression (14, 33, 34). It is likely that elevated ODC activity in primary cultures of proliferating keratinocytes is a greater stress than in relatively quiescent keratinocytes in intact skin. Although ATM is activated and p53 levels accumulate in both ODC-overexpressing keratinocyte cultures and in ODC transgenic skin, massive apoptosis is only observed in Ker/ODC cultured at subconfluent density. Thus, p53-dependent apoptotic cell death eliminates cells that have acquired ROS-induced damage that is too severe to be repairable or that may be oncogenic. Because ODC-overexpressing keratinocytes exhibit both increased ROS production as well as increased DNA damage, ODC-induced apoptosis of cells with a functional p53 may play an important role in promoting tumorigenesis by contributing to a mutator phenotype. Indeed, Wallon et al. (38) reported that overexpression of ODC enzyme targeted to the skin of K6/ODC transgenic mice may increase susceptibility to mutation following carcinogen exposure. In addition, recent studies have shown that whereas DNA damage induction of p53 can produce a strong apoptotic response, it is not necessary for p53-mediated tumor suppression, which requires ARF signaling in response to oncogene activation (7, 39). Thus, the lack of signaling through the ARF pathway, which is critical for p53-mediated tumor suppression, may leave the tissue more susceptible to genetic instability and tumor progression.

With increased ODC activity, stimulation of polyamine biosynthesis and subsequent increased intracellular polyamine levels induce the activity of normal polyamine catabolic pathways. We have shown that elevated ODC activity in normal keratinocytes results in the early induction of SMO that generates both 3-aminopropanal/acrolein and H_2O_2, leads to increased DNA damage, and activates ATM signaling. This novel activation of ATM and stabilization of p53 is dependent on polyamine biosynthesis because specific inhibition of ODC activity with DFMO prevents both the generation of ROS and the subsequent activation of the ATM-DNA damage response pathway. Moreover, inhibition of SMO activity with MDL 72,527 treatment also inhibits ROS generation and subsequent cell death in ODC-overexpressing keratinocytes. We found no evidence for ODC induction of polyamine catabolism via the SSAT/APAO pathway because there was no increase in SSAT activity, no acetylated polyamines detected, and no increase in APAO mRNA or protein levels in Ker/ODC. Indeed, a recent report (6) that SSAT overexpression leads to DNA damage and G_2 arrest concluded that the primary driving mechanism was due to the depletion of cellular polyamines with increased H_2O_2 production, playing only a secondary role in the reduced cell proliferation. Furthermore, they found that SMO activity was not induced with SSAT overexpression, and the cells did not undergo apoptotic cell death despite the presence of damaged DNA (6). The decreased spermine levels detected in ODC-overexpressing keratinocytes and skin likely results from the increased SMO activity. Although increased activity of polyamine catabolic oxidases, including both APAO and SMO, have been shown to lead to oxidative stress (21, 22, 25), our data suggest that induction of SMO is primarily responsible for the increased H_2O_2 and acrolein accumulation in Ker/ODC. Igarashi et al. (28, 40) have shown that acrolein is the major toxic compound produced from spermine by SMO. We have shown by a direct ELISA assay that there is a significant increase in acrolein-conjugated lysine in Ker/ODC cell lysates compared with Ker/Norm and that this can be blocked with DFMO. Because acrolein has been reported to cause DNA damage and cell damage in a variety of cell types (40, 41), it is likely that both H_2O_2 and aldehyde/acrolein produced via SMO activity are responsible for the induction of the DNA damage response observed in keratinocytes with elevated ODC activity.

Previous reports have also shown that alterations in intracellular polyamine levels can lead to apoptotic cell death. In particular, accumulation of putrescine, as a result of increased ODC activity or increased uptake from the medium, can provoke apoptosis in various cell types (42, 43). Putrescine induction of oxidative stress has been implicated to mediate apoptotic cell death induced by ODC (44), but the signaling pathways involved have not been defined before this study. Conversely, DFMO depletion of polyamines has also been reported by Li et al.(45) to induce *p53* gene expression and growth inhibition but not apoptosis in intestinal epithelial cells. Similarly, treatment of cells with polyamine analogues also results in decreased intracellular polyamines but, in some cases, cells undergo apoptosis (46, 47). However, unlike DFMO depletion of polyamines, polyamine analogues induce the activity of polyamine catabolic enzymes, including SMO and polyamine oxidase, that generate H_2O_2 and toxic aldehyde/acrolein (21, 28, 48). The induction of polyamine catabolic oxidases and its associated H_2O_2 generation seems to be responsible for the antitumor activity of a variety of polyamine analogues (21). We have observed that treatment of ODC-overexpressing primary keratinocytes with the polyamine analogues, BENSpm or CPENSpm, accelerates their apoptotic cell death (data not shown). Thus, ODC-overexpressing keratinocytes are more sensitive to agents, such as the polyamine analogues, that cause additional ROS generation.

In summary, we show that apoptotic cell death is induced in normal keratinocytes with elevated ODC activity via the induced generation of reactive aldehydes and H_2O_2, at least in part due to induction of SMO, followed by the subsequent activation of the ATM-DNA damage response pathway. Because elevated ODC is a common characteristic of tumor cells, it is possible that cells with high ODC activity will be selectively sensitized to die when exposed to further oxidative insults by radiation or agents that cause further ROS stress. On the other hand, further studies are needed to explore the possibility that ODC up-regulation of polyamine catabolic oxidation and production of mutagenic ROS contributes to a malignant phenotype. Recent studies have shown that ROS production by inflammatory cells and its association with tumor development seems to be mediated in some cases by the induction of SMO either in response to pathogens such as *Helicobacter pylori* (49) or via a direct induction of SMO by tumor necrosis factor α

(50). Accordingly, SMO may be a promising target for antineoplastic intervention in premalignant tissue with elevated ODC activity.

Acknowledgments

Received 8/24/2007; revised 12/6/2007; accepted 12/28/2007.
Grant support: NIH grants CA95592 and CA70739 (S.K. Gilmour).

The costs of publication of this article were defrayed in part by the payment of page charges. This article must therefore be hereby marked *advertisement* in accordance with 18 U.S.C. Section 1734 solely to indicate this fact.

We thank Dr. Robert Casero for his generous gift of SMO antibody and for his many insightful suggestions; Dr. Slavoljub Vujcic and Paula Diegelman for their excellent technical assistance; Drs. Debora Kramer, Ira Ayene, and Alex Muller for helpful discussions and valuable comments on the manuscript; and Kate Ciavarelli for editorial assistance.

References

1. Gilmour SK, Birchler M, Smith MK, Rayca K, Mostochuk J. Effect of elevated levels of ornithine decarboxylase on cell cycle progression in skin. Cell Growth Differ 1999;10:739–48.
2. O'Brien TG, Megosh LC, Gilliard G, Soler AP. Ornithine decarboxylase overexpression is a sufficient condition for tumor promotion in mouse skin. Cancer Res 1997;57:2630–7.
3. Smith MK, Trempus CS, Gilmour SK. Co-operation between follicular ornithine decarboxylase and v-Ha-ras induces spontaneous papillomas and malignant conversion in transgenic skin. Carcinogenesis 1998;19:1409–15.
4. Ray RM, Zimmerman BJ, McCormack SA, Patel TB, Johnson LR. Polyamine depletion arrests cell cycle and induces inhibitors p21(Waf1/Cip1), p27(Kip1), and p53 in IEC-6 cells. Am J Physiol 1999;276:C684–91.
5. Kramer DL, Vujcic S, Diegelman P, et al. Polyamine analogue induction of the p53-21WAF1/CIP1-Rb pathway and G1 arrest in human melanoma cells. Cancer Res 1999;59:1278–86.
6. Zahedi K, Bissler JJ, Wang Z, et al. Spermidine/spermine N^1-acetyltransferase overexpression in kidney epithelial cells disrupts polyamine homeostasis, leads to DNA damage, and causes G_2 arrest. Am J Physiol Cell Physiol 2007;292:C1204–15.
7. Efeyan A, Serrano M. p53: guardian of the genome and policeman of the oncogenes. Cell Cycle 2007;6:1006–10.
8. Prives C, Hall PA. The p53 pathway. J Pathol 1999;187:112–26.
9. Hollstein M, Shomer B, Greenblatt M, et al. Somatic point mutations in the p53 gene of human tumors and cell lines: updated compilation. Nucleic Acids Res 1996;24:141–6.
10. Bakkenist CJ, Kastan MB. Initiating cellular stress responses. Cell 2004;118:9–17.
11. Appella E, Anderson CW. Post-translational modifications and activation of p53 by genotoxic stresses. Eur J Biochem 2001;268:2764–72.
12. Kang J, Ferguson D, Song H, et al. Functional interaction of H2AX, NBS1, and p53 in ATM-dependent DNA damage responses and tumor suppression. Mol Cell Biol 2005;25:661–70.
13. Vafa O, Wade M, Kern S, et al. c-Myc can induce DNA damage, increase reactive oxygen species, and mitigate p53 function: a mechanism for oncogene-induced genetic instability. Mol Cell 2002;9:1031–44.
14. Hong S, Pusapati RV, Powers JT, Johnson DG. Oncogenes and the DNA damage response: Myc and E2F1 engage the ATM signaling pathway to activate p53 and induce apoptosis. Cell Cycle 2006;5:801–3.
15. Pusapati RV, Rounbehler RJ, Hong S, et al. ATM promotes apoptosis and suppresses tumorigenesis in response to Myc. Proc Natl Acad Sci U S A 2006;103:1446–51.
16. Lan L, Hayes CS, Laury-Kleintop L, Gilmour S. Suprabasal induction of ornithine decarboxylase in adult mouse skin is sufficient to activate keratinocytes. J Invest Dermatol 2005;124:602–14.
17. Brooks CL, Gu W. Ubiquitination, phosphorylation and acetylation: the molecular basis for p53 regulation. Curr Opin Cell Biol 2003;15:164–71.
18. Banin S, Moyal L, Shieh S, et al. Enhanced phosphorylation of p53 by ATM in response to DNA damage. Science 1998;281:1674–7.
19. Sherr CJ. The INK4a/ARF network in tumour suppression. Nat Rev Mol Cell Biol 2001;2:731–7.
20. Rogakou EP, Pilch DR, Orr AH, Ivanova VS, Bonner WM. DNA double-stranded breaks induce histone H2AX phosphorylation on serine 139. J Biol Chem 1998;273:5858–68.
21. Pledgie A, Huang Y, Hacker A, et al. Spermine oxidase SMO(PAOh1), Not N^1-acetylpolyamine oxidase PAO, is the primary source of cytotoxic H_2O_2 in polyamine analogue-treated human breast cancer cell lines. J Biol Chem 2005;280:39843–51.
22. Vujcic S, Diegelman P, Bacchi CJ, Kramer DL, Porter CW. Identification and characterization of a novel flavin-containing spermine oxidase of mammalian cell origin. Biochem J 2002;367:665–75.
23. Vujcic S, Liang P, Diegelman P, Kramer DL, Porter CW. Genomic identification and biochemical characterization of the mammalian polyamine oxidase involved in polyamine back-conversion. Biochem J 2003;370:19–28.
24. Wang Y, Devereux W, Woster PM, Stewart TM, Hacker A, Casero RA, Jr. Cloning and characterization of a human polyamine oxidase that is inducible by polyamine analogue exposure. Cancer Res 2001;61:5370–3.
25. Wang Y, Murray-Stewart T, Devereux W, et al. Properties of purified recombinant human polyamine oxidase, PAOh1/SMO. Biochem Biophys Res Commun 2003;304:605–11.
26. Barzilai A, Yamamoto K. DNA damage responses to oxidative stress. DNA Repair Amst 2004;3:1109–15.
27. Tanaka T, Halicka HD, Huang X, Traganos F, Darzynkiewicz Z. Constitutive histone H2AX phosphorylation and ATM activation, the reporters of DNA damage by endogenous oxidants. Cell Cycle 2006;5:1940–5.
28. Sakata K, Kashiwagi K, Sharmin S, Ueda S, Igarashi K. Acrolein produced from polyamines as one of the uraemic toxins. Biochem Soc Trans 2003;31:371–4.
29. Bakkenist CJ, Kastan MB. DNA damage activates ATM through intermolecular autophosphorylation and dimer dissociation. Nature 2003;421:499–506.
30. Sun Y, Jiang X, Chen S, Fernandes N, Price BD. A role for the Tip60 histone acetyltransferase in the acetylation and activation of ATM. Proc Natl Acad Sci U S A 2005;102:13182–7.
31. Hobbs CA, Wei G, Defeo K, Paul B, Hayes CS, Gilmour SK. Tip60 protein isoforms and altered function in skin and tumors that overexpress ornithine decarboxylase. Cancer Res 2006;66:8116–22.
32. Bello-Fernandez C, Packham G, Cleveland JL. The ornithine decarboxylase gene is a transcriptional target of c-Myc. Proc Natl Acad Sci U S A 1993;90:7804–8.
33. Bartkova J, Horejsi Z, Koed K, et al. DNA damage response as a candidate anti-cancer barrier in early human tumorigenesis. Nature 2005;434:864–70.
34. Gorgoulis VG, Vassiliou LV, Karakaidos P, et al. Activation of the DNA damage checkpoint and genomic instability in human precancerous lesions. Nature 2005;434:907–13.
35. Di Micco R, Fumagalli M, Cicalese A, et al. Oncogene-induced senescence is a DNA damage response triggered by DNA hyper-replication. Nature 2006;444:638–42.
36. Lee AC, Fenster BE, Ito H, et al. Ras proteins induce senescence by altering the intracellular levels of reactive oxygen species. J Biol Chem 1999;274:7936–40.
37. Zhao Y, Chaiswing L, Bakthavatchalu V, Oberley TD, St Clair DK. Ras mutation promotes p53 activation and apoptosis of skin keratinocytes. Carcinogenesis 2006;27:1692–8.
38. Wallon UM, O'Brien T G. Polyamines modulate carcinogen-induced mutagenesis *in vivo*. Environ Mol Mutagen 2005;45:62–9.
39. Christophorou MA, Ringshausen I, Finch AJ, Swigart LB, Evan GI. The pathological response to DNA damage does not contribute to p53-mediated tumour suppression. Nature 2006;443:214–7.
40. Igarashi K, Ueda S, Yoshida K, Kashiwagi K. Polyamines in renal failure. Amino Acids 2006;31:477–83.
41. Feng Z, Hu W, Hu Y, Tang MS. Acrolein is a major cigarette-related lung cancer agent: Preferential binding at p53 mutational hotspots and inhibition of DNA repair. Proc Natl Acad Sci U S A 2006;103:15404–9.
42. Tobias KE, Kahana C. Exposure to ornithine results in excessive accumulation of putrescine and apoptotic cell death in ornithine decarboxylase overproducing mouse myeloma cells. Cell Growth Differ 1995;6:1279–85.
43. Tome ME, Fiser SM, Payne CM, Gerner EW. Excess putrescine accumulation inhibits the formation of modified eukaryotic initiation factor 5A (eIF-5A) and induces apoptosis. Biochem J 1997;328:847–54.
44. Erez O, Goldstaub D, Friedman J, Kahana C. Putrescine activates oxidative stress dependent apoptotic death in ornithine decarboxylase overproducing mouse myeloma cells. Exp Cell Res 2002;281:148–56.
45. Li L, Li J, Rao JN, Li M, Bass BL, Wang JY. Inhibition of polyamine synthesis induces p53 gene expression but not apoptosis. Am J Physiol 1999;276:C946–54.
46. Kramer DL, Fogel-Petrovic M, Miller J, et al. Effects of novel spermine analogs on cell cycle progression and apoptosis in MALME-3M human melanoma cells. Cancer Res 1997;57:5521–7.
47. Casero RA, Jr., Frydman B, Stewart TM, Woster PM. Significance of targeting polyamine metabolism as an antineoplastic strategy: unique targets for polyamine analogues. Proc West Pharmacol Soc 2005;48:24–30.
48. Devereux W, Wang Y, Stewart TM, et al. Induction of the PAOh1/SMO polyamine oxidase by polyamine analogues in human lung carcinoma cells. Cancer Chemother Pharmacol 2003;52:383–90.
49. Xu H, Chaturvedi R, Cheng Y, et al. Spermine oxidation induced by Helicobacter pylori results in apoptosis and DNA damage: implications for gastric carcinogenesis. Cancer Res 2004;64:8521–5.
50. Babbar N, Casero RA, Jr. Tumor necrosis factor-α increases reactive oxygen species by inducing spermine oxidase in human lung epithelial cells: a potential mechanism for inflammation-induced carcinogenesis. Cancer Res 2006;66:11125–30.